Determination of the phase of magneto-intersubband scattering oscillations in heterojunctions and quantum wells

T. H. Sander,* S. N. Holmes,† and J. J. Harris‡
IRC Semiconductor Materials, Imperial College, London SW7 2BZ, United Kingdom

D. K. Maude and J. C. Portal
CNRS, Laboratoire des Champs Magnetiques Intenses, BP 166, 38042 Grenoble, France
(Received 11 March 1998; revised manuscript received 8 July 1998)

The oscillatory magnetoresistance of a two-dimensional electron system with two occupied subbands has been studied in an $Al_{0.3}Ga_{0.7}As/GaAs$ heterojunction and an $Al_{0.3}Ga_{0.7}As/In_{0.15}Ga_{0.85}As/GaAs$ quantum well between 4 and 100 K. As a consequence of the second populated subband, a magneto-intersubband scattering effect is observed at low-magnetic fields in addition to the Shubnikov–de Haas effect. Due to the different temperature damping of the two effects, the oscillatory magnetoresistance can exhibit both effects simultaneously at high and respectively low fields. Using the extrema positions, it is possible to clearly identify a theoretically predicted phase difference between the Shubnikov–de Haas and the magneto-intersubband scattering oscillations at temperatures higher than 4 K. This phase difference influences the power spectrum of reciprocal-field magnetoresistance data. [S0163-1829(98)04444-0]

I. INTRODUCTION

The Shubnikov–de Haas (SdH) effect is widely used to characterize two-dimensional electron systems (2DES) in semiconductor heterojunctions. When a single electric subband is populated the SdH oscillations in the magnetoresistance have a simple mathematical form.[1] For some time $Al_{0.3}Ga_{0.7}As/GaAs$ and related heterojunctions have been grown, which have two populated subbands at 4 K or above. Typical transport experiments on such samples can be found in Refs. 2 and 3.

Only recently it was discovered experimentally and theoretically[4–7] that the oscillatory magnetoresistance of a high mobility 2DES with two populated subbands contains at least three components: the SdH oscillations of the two subbands and an oscillation due to elastic scattering between the subbands. This third component was termed the magneto-intersubband scattering (MIS) effect by Raikh and Shahbazyan.[6] This dominates the oscillatory magnetoresistance upon increasing the temperature above 4 K due to its weak-temperature damping compared to SdH oscillations. The fundamental field of the MIS oscillations is a measure of the subband spacing in the 2DES assuming a subband independent effective mass.[7]

Below a certain field limit the SdH and MIS oscillations are described by a cosine function multiplied by a nonoscillatory damping term, which is magnetic field and temperature dependent for the SdH oscillations and only field dependent for the MIS oscillations. The two different theoretical approaches of Refs. 5 and 6 predict both a phase difference of $\Delta\phi=\pi$ between the cosine terms of the SdH and MIS oscillations.

Magnetoresistance data obtained by Leadley *et al.*[5] from $Al_{0.3}Ga_{0.7}As/GaAs$ heterojunctions indicate $\Delta\phi\approx\pi$ between SdH and MIS oscillations below 4 K. A detailed phase analysis of the thermopower[8] for several $Al_{0.3}Ga_{0.7}As/GaAs$ heterojunctions below 4 K demonstrates a more complex behavior than the transport results.[5]

By studying the temperature range above 4 K, we are able to identify the phase difference between SdH and MIS oscillations unambiguously in the magnetoresistance. The direct identification of the phase difference is possible due to the different field and temperature damping behavior of SdH and MIS oscillations. At typically 20 K the magnetoresistance is dominated in the low-field regime by MIS and in the high-field regime by SdH oscillations. Then the phase difference can be deduced from the extrema positions of the oscillatory magnetoresistance. The experimental results of the first sample, a pseudomorphic $Al_xGa_{1-x}As/In_xGa_{1-x}As/GaAs$ modulation-doped structure, show the phase difference in unprocessed magnetoresistance data due to identical SdH and MIS fundamental fields. The second sample, an $Al_xGa_{1-x}As/GaAs$ heterojunction similar to that given an initial study above 4 K,[9] corresponds to the typical case, where the SdH and MIS fundamental fields are different.

The calculation of the power spectrum of the Fourier transform is a standard tool in the analysis of experimental SdH magnetoresistance data of 2DES's.[5,9–11] Determining the carrier concentration from the peaks in the spectra is of great experimental importance. We show that the phase difference introduces uncertainties into the power spectrum.

II. MAGNETO-INTERSUBBAND SCATTERING AND SHUBNIKOV de–HAAS THEORY

The effect of elastic-intersubband scattering on the SdH oscillations of a two-subband 2DES has been studied theoretically, using inversion of the two-subband conductivity tensor,[4,5] and a Kubo formalism.[6] The two different approaches predict an additional oscillatory component in the magnetoresistance. This MIS effect is due to increased elastic-intersubband scattering at subband Landau-level crossover. This crossover occurs for a parabolic subband dis-

persion at magnetic fields given by

$$B=\frac{E_{12}m^*}{\hbar e(l_1-l_2)}, \tag{2.1}$$

where $E_{12}=E_2-E_1$ is the subband spacing, the l_i are the Landau-level indices of the lowest $(i=1)$ and the first-excited (second) subband $(i=2)$. The indices l_i fulfill the relation $l_1-l_2>0$ as the lth Landau level of the lower subband can never cross the corresponding Landau level of the second subband. For the experiment, it is convenient to define $B_{f,MIS}\equiv E_{12}m^*/\hbar e$, the MIS fundamental field. Note that Eq. (2.1) is identical to the relation between the Fermi energy $E_{F,i}$ and the magnetoresistance extrema positions due to the SdH effect, when replacing E_{12} by $E_{F,i}=E_F-E_i$ $(i=1,2)$ and the difference l_1-l_2 by the filling factor ν. Using the relation between $E_{F,i}$ and the carrier density $n_{s,i}$ of each subband of the 2DES, the SdH fundamental field is defined as $B_{f,SdH,i}=hn_{s,i}/2e$.

Leadley *et al.* and Coleridge[4,5] extended the energy-dependent conductivity tensor suggested in Ref. 1 to two subbands. After inverting this tensor and averaging with the Fermi-Dirac function, the following equation is obtained, which is strictly applicable at low-magnetic fields and low temperatures:

$$\frac{\Delta\rho_{xx}}{\rho_0}=2A_1\frac{X}{\sinh X}\exp\left(-\frac{\pi}{\omega_c\tau_1}\right)\cos\left[\frac{2\pi(E_F-E_1)}{\hbar\omega_c}+\pi\right] \tag{2.2a}$$

$$+2A_2\frac{X}{\sinh X}\exp\left(-\frac{\pi}{\omega_c\tau_2}\right)\cos\left[\frac{2\pi(E_F-E_2)}{\hbar\omega_c}+\pi\right] \tag{2.2b}$$

$$+2B_{12}\frac{2X}{\sinh 2X}\exp\left[-\frac{\pi}{\omega_c}\left(\frac{1}{\tau_1}+\frac{1}{\tau_2}\right)\right]\times\cos\left[\frac{2\pi(2E_F-E_1-E_2)}{\hbar\omega_c}\right] \tag{2.2c}$$

$$+2B_{12}\exp\left[-\frac{\pi}{\omega_c}\left(\frac{1}{\tau_1}+\frac{1}{\tau_2}\right)\right]\cos\left(\frac{2\pi E_{12}}{\hbar\omega_c}\right). \tag{2.2d}$$

The amplitude factors A_1, A_2, and B_{12} are related to the intrasubband and intersubband scattering probabilities P_{ij} $(i,j=1,2)$ and $X=2\pi^2K_BT/\hbar\omega_c$. The first two terms Eqs. (2.2a) and (2.2b) are the typical SdH terms in the presence of two subbands. The third term, Eq. (2.2c), contains the temperature damping factor $2X/\sinh(2X)$, which leads to a temperature damping much stronger than that of the SdH terms. The fourth term, Eq. (2.2d), is the MIS term. It does not contain the thermal damping factor $X/\sinh(X)$ and the fundamental field is proportional to the subband spacing, E_{12}.

Using the relation $A_i>B_{12}$ (Ref. 5) and assuming that the amplitude factors in Eqs. (2.2) do not differ by several orders of magnitude, it can be easily verified that the different thermal damping behavior of the SdH and MIS terms leads to three temperature regimes in the magnetoresistance. At low temperatures, the SdH terms dominate and at high temperatures the MIS term. At intermediate temperatures the oscillatory magnetoresistance is split into a low- and high-field regime, the MIS term is dominant below a certain field and the SdH terms above that field. The SdH terms Eqs. (2.2a) and (2.2b) and the MIS term Eq. (2.2d) have a phase difference $\Delta\phi=\pi$, i.e., have a different sign as the amplitude factors A_1, A_2, and B_{12} are positive. It is interesting to consider the case $B_{f,SdH,1}\approx B_{f,MIS}$ in Eqs. (2.2a) and (2.2d). At a certain field B_{node} the amplitude of the SdH and MIS terms will be equal and due to the phase difference destructive interference should occur. Above and below B_{node} the amplitudes are different and therefore the extinction of the oscillation will be incomplete. Nevertheless a clear node in the oscillation envelope is expected. For $B_{f,SdH,1}\neq B_{f,MIS}$ the node will become weaker as the difference between the two fundamental fields increases.

The phase difference can be understood by simple arguments. If the Fermi level is exactly between Landau levels an integer number n of Landau levels is filled, corresponding to $(E_F-E_1)/\hbar\omega_c=n$ with $n>0$ and assuming spin degeneracy. At these fields the resistance caused by elastic *intrasubband* scattering has a minimum due to a minimum in the density of final states. This corresponds to the phase $\phi=\pi$ in the cosine of the SdH terms. At subband Landau-level crossover, i.e., at $E_{12}/\hbar\omega_c=n$, the elastic *intersubband* scattering channel opens up and the resistance has a local maximum. Therefore, the phase is zero in the cosine of the MIS term.

In a thorough theoretical treatment, Raikh and Shahbazyan[6] calculate the oscillatory magnetoconductivity of a two-subband 2DES for the case of delta function scatterers and a highly populated second subband. Besides the usual SdH terms for each subband, terms similar to Eqs. (2.2c) and (2.2d) are obtained. Additionally, a temperature-independent prefactor of the MIS term is derived in Ref. 6. Unfortunately, this theory is not applicable in our experimental situation as the second subband is not highly populated.

III. EXPERIMENTAL PROCEDURE

The transport experiments described in this paper were performed on two samples grown by molecular-beam epitaxy at Philips (Redhill, UK), which were processed into standard Hall bars by photolithography. Sample *A* was a modulation-doped pseudomorphic $Al_{0.3}Ga_{0.7}As/In_{0.15}Ga_{0.85}As/GaAs$ heterojunction with a well width of 15 nm and a spacer width of 7.5 nm, sample B was a modulation-doped $Al_{0.3}Ga_{0.7}As/GaAs$ heterojunction with a spacer width of 2.5 nm. At 4 K, sample *A* had a carrier concentration $n_s=1.41\times10^{12}\,\mathrm{cm}^{-2}$ and a mobility $\mu=6\,\mathrm{m}^2/\mathrm{V\,s}$. Sample *B* had $n_s=1.13\times10^{12}\,\mathrm{cm}^{-2}$ and $\mu=16\,\mathrm{m}^2/\mathrm{V\,s}$. The densities were determined from $B_{f,SdH,1}$ of the extrema-index plots given in Table I and the mobilities from the Hall effect and the zero-field resistivity. The density of the second subband for sample *B* is about $1.0\times10^{11}\,\mathrm{cm}^{-2}$ and it has been neglected together with the resulting uncertainty in the Hall factor in determining n_s and μ. Prior to the measurements the samples were cooled in the dark to 4 K, briefly illuminated with infrared radiation, and then left in the dark to reach equilibrium as monitored by the resistance.[3] Then a series of magnetoresistance traces was taken at successively higher temperatures.

Experimental magnetoresistance data are usually a combi-

TABLE I. Comparison between the fundamental field values B_f determined from the power spectra and the extrema-index plots.

	Power spectrum		Extrema-index plot	
T (K)	$B_{f,SdH,1}$ (T)	$B_{f,MIS}$ (T)	$B_{f,SdH,1}$ (T)	$B_{f,MIS}$ (T)
		Sample *A*		
4	29.2		29.3	
20	28.0	30.7	28.9	29.2
30	27.5	31.2	27.9	28.9
50		27.5		28.9
100		29.7		28.9
		Sample *B*		
4	23.4	21.2	23.6	
10	23.4	21.2	23.7	21.5
20		21.4		21.4
50				23.3
90				22.2

nation of a slowly varying background and an oscillatory component. In our samples the background resistance is caused by parallel conduction due to the high doping levels. To facilitate the analysis of the oscillatory component, we calculate the first derivative of the experimental data as is shown in Fig. 1. We compare these data with the theory discussed above and therefore the derivatives of the theoretical expressions Eqs. (2.2a) and (2.2d), the SdH and MIS terms, have to be considered. The derivative of Eq. (2.2a) consists of three terms due to the three factors $a/B\sinh(a/B)$, $\exp(-b/B)$, and $\cos(c/B+\pi)$, where $a=2\pi^2K_Bm^*T/\hbar e$, $b=\pi m^*/e\tau_1$, and $c=2\pi(E_F-E_1)m^*/\hbar e$. As can be easily verified the dominant term in the derivative is determined by the relative magnitude of the parameters a to c. One finds $a\approx T$ using $m^*=0.067m_e$ for GaAs, $b\approx 12$ using $\tau_1=0.1$ ps. This quantum lifetime value is a lower bound estimated from the mobility values given above using the typical ratio of 10 between the transport and the quantum lifetime.[12] One obtains $c\approx 70$ using $E_F-E_1=20$ meV as a reasonable lower bound for our high-carrier density samples. Therefore even at high temperatures the derivative of Eq. (2.2a) is essentially $(c/B^2)[a/B\sinh(a/B)]\exp(-b/B)\sin(c/B+\pi)$. The result for Eq. (2.2d) is similar, although without the damping term. As the derivatives of Eqs. (2.2a) and (2.2d) are dominated by sine terms the extrema in the first derivative are shifted by approximately $\pi/2$ compared to the undifferentiated expressions, nevertheless, the phase difference $\Delta\phi=\pi$ between MIS and SdH term is essentially preserved. The factor $1/B^2$ in the first derivative enhances the oscillations at low fields and the observation of MIS oscillations is easier.

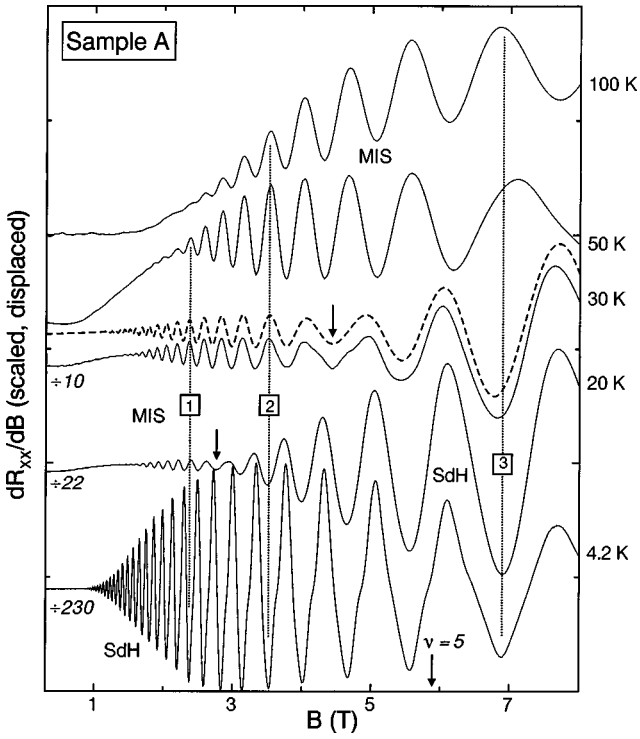

FIG. 1. The first derivative of the magnetoresistance of sample *A* as a function of temperature. Note the nodes (arrows) and the alignment of the minima and maxima as a function of temperature (vertical dotted lines). A best approximation to the data at 30 K using Eqs. (2.2a) and (2.2d) is shown as the dashed line. The curves are scaled as indicated.

We use two methods to obtain the fundamental field B_f of oscillatory magnetoresistance data periodic with respect to inverse field. The first uses directly the positions of the magnetoresistance extrema, in an extrema-index plot. Equation (2.1) can be rewritten as $N=B_f/B_N+\phi/\pi$, where $N=l_1-l_2$, B_N is the magnetic field position of a resistance maximum, and ϕ/π is the phase in cycles. The slope of this linear relationship is directly the value of B_f. Therefore, the measurement of the positions of the MIS or equivalently the SdH maxima is sufficient to obtain B_f from a linear fit to the $(N,1/B_N)$ data set.[13,14] A phase ϕ was not included in Eq. (2.1) as it is ideally zero for MIS oscillations. Now it is nonzero as $\phi=\pi/2$ or $-\pi/2$ is expected in the derivative of MIS and SdH oscillations. Using the value of B_f determined from the extrema-index plot it is possible to determine the phase ϕ in a residual-phase plot, where $\phi/\pi=N-B_f/B_N$ is plotted as a function of $1/B_N$. For the correct B_f this plot gives a constant value and the phase can be determined by extrapolation to zero. For simple sine-wave oscillations both maxima and minima can be used to determine B_f, the slope is then $2B_f$. An example of an extrema-index and a residual-phase plot using all extrema is shown in Fig. 2. The second method is the Fast Fourier transform algorithm[15] and the subsequent calculation of the power spectral density. It shows all the harmonic content in a single curve, but the phase information is lost. Examples of power spectra can be seen in Fig. 3.

IV. RESULTS AND DISCUSSION

A. Magnetoresistance of sample *A*

We will now discuss the experimental results for sample *A*, the $Al_{0.3}Ga_{0.7}As/In_{0.15}Ga_{0.85}As/GaAs$ quantum well. This sample has only one occupied subband upon cooling in the dark as deduced from SdH oscillations. After cooling, the carrier concentration of the sample was slowly increased by stepwise illumination until the special condition $E_{F,1}\approx E_{12}$ was achieved, i.e., $B_{f,SdH,1}\approx B_{f,MIS}$. Only the data set corresponding to this condition is discussed. It enables the iden-

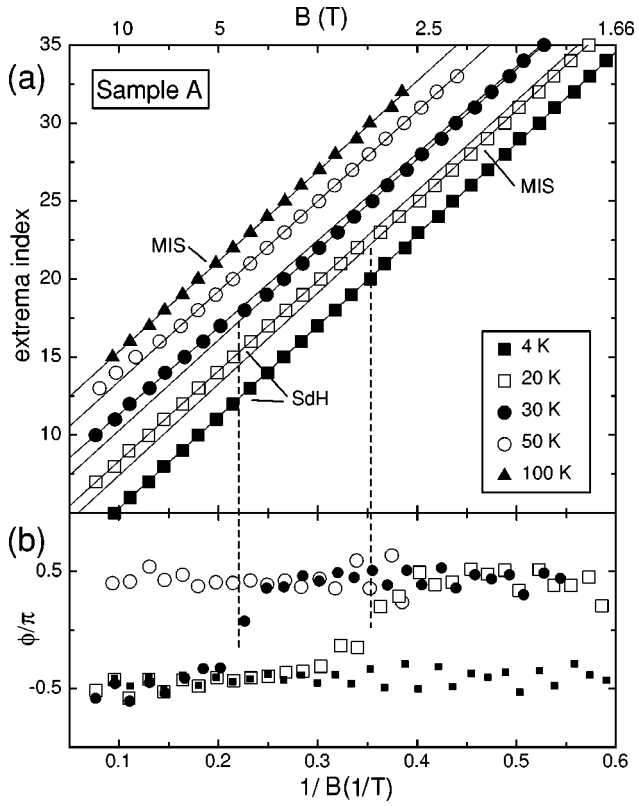

FIG. 2. The extrema-index (a) and residual-phase (b) plots for sample *A*. The slope in (a), i.e., the fundamental field, is almost independent of temperature. Well-pronounced discontinuities occur in the plots at 20 and 30 K. The fundamental fields derived from the slopes are given in Table I. In (b) a phase shift of π is observed occurring at the positions of the discontinuities in (a) as indicated by the dashed-vertical line.

tification of the phase difference $\Delta\phi$ between MIS and SdH peaks in the magnetoresistance without further manipulation and for $\Delta\phi=\pi$ a strong interference node is expected in the oscillation envelope.

The first derivative of the magnetoresistance for sample *A* after controlled illumination is shown in Fig. 1. The solid lines are measured data, the dashed line is an approximation to be discussed later. The curves at 4, 20, and 30 K are scaled with the factors given. At 4 K, SdH oscillations typical of a single subband are observed. This is not a contradiction to the condition $E_{F,1}\approx E_{12}$, which is equivalent to a weakly populated second subband at 4 K. For reference the location of the filling factor $\nu=5$ of the lowest subband is indicated. Its position has to be between a minimum and a maximum as first derivative data are shown.

At 20 and 30 K, nodes are observed at $B_{node}=3$ and 4.5 T as indicated by the arrows. To study the phase relation between the extrema positions as a function of temperature three vertical dotted lines, labeled 1 to 3, are drawn on the graph. The positions of all three lines are chosen to intersect a minimum of the curve at 4 K. Already at 20 K the situation has changed as line 1 intersects a maximum and the node is between line 1 and 2. At 30 K the node is between line 2 and 3 and they intersect a maximum and a minimum, respectively. At 50 K all three lines intersect a maximum. The number of minima between line 1 and 3 at 4 K is seven, as is the number of maxima at 50 K between the two lines. This

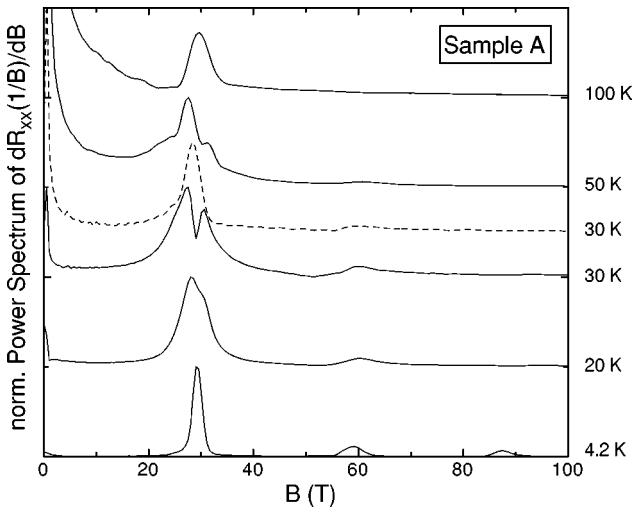

FIG. 3. The normalized power spectra for sample *A*. The vertical line was added to show the relative position of the peaks, note the double peak at 30 K. The dashed line shows a spectrum of the 30 K data for a field range limited to $B<4.5$ T. A single peak remains.

means the fundamental field is the same at 4 and 50 K, although the phase has changed by π. Such a phase difference and the occurrence of nodes cannot be explained by single subband SdH oscillations.

Interpreting the data at 30 K in Fig. 1 at low fields as MIS and at high fields as SdH oscillations we approximated the experimental data using the appropriate theoretical curve, which is the derivative of Eqs. (2.2a) and (2.2d) with a variable phase $\delta\phi\approx n\pi$, where $n=0,1,2,\ldots$. This approximation is the dashed curve and it indeed reproduces the measured data very well. The values for the MIS term Eq. (2.2d) dominant at low fields are $B_f=29.0$ T and $\delta\phi=6.13$, $B_f=28.2$ T and $\delta\phi=3.53$ belong to the SdH term Eq. (2.2a) dominant at high fields. The fundamental fields are close to each other and a $\Delta\phi=6.13-3.53=2.60$ closer to π than to zero is found in agreement with the simple analysis using the points of intersection of the lines 1 to 3.

Estimating the thermal damping of the SdH oscillations Eq. (2.2a) using the parameters discussed in a Sec. III it is found that the oscillation amplitude in Fig. 1 below the nodes is far too large for the SdH effect. The movement of the node to higher fields with increasing temperature can be explained by the stronger temperature damping of SdH in comparison with MIS oscillations. We conclude that the oscillatory magnetoresistance at 20 and 30 K is dominated below the node by MIS and above the node by the SdH effect. At 4 K only SdH and at 50 K only MIS oscillations occur in the field range considered.

B. Fundamental fields and phases of sample *A*

To determine the fundamental fields and phases of the curves in Fig. 1, the corresponding extrema-index and residual-phase plots are shown in Fig. 2, which does not include the extrema positions observed at the lowest and highest fields to emphasize the middle section. The data sets are vertically displaced for clarity.

At 4 K all points are on a straight line as indicated by the linear fit in Fig. 2(a) and the slope gives $B_{f,SdH}$. At 20 K the

data set shows a discontinuity at $1/B \approx 0.35\ \mathrm{T}^{-1}$. This discontinuity is not caused by the random omission of an extrema, care was taken to include all extrema of the magnetoresistance curve. The discontinuity coincides with B_{node} at 20 K in the magnetoresistance data in Fig. 1 (since 1/0.35 $=2.86$ T). The regions below and above the discontinuity show linear behavior and have almost the same slope. Again we assign the low-field oscillations below the nodes to the MIS effect and therefore the slope at large $1/B$ is associated with $B_{f,MIS}$ and at small $1/B$ with $B_{f,SdH,1}$. At 30 K the behavior is similar, although slightly different fundamental fields are observed below and above the discontinuity. The position of the discontinuity has moved to lower $1/B$ compared to the plot at 20 K in agreement with B_{node} in the curve at 30 K in Fig. 1. At 50 K, only a few extrema do not fit onto the straight line. These extrema are outside the field range of Fig. 1 and the node is not visible. At 100 K all points are on a straight line. The resulting values are given in Table I.

Figure 2(b) shows the residual-phase plots between 4 and 50 K using the B_f-values obtained in Fig. 2(a), $B_{f,SdH,1}$ is used at 4 K and $B_{f,MIS}$ above that. At 4 K, the phase is $\phi = -\pi/2$ as expected for the first derivative of SdH oscillations. At 20 and 30 K, the phase jumps from $-\pi/2$ to $\pi/2$ at the same positions, where discontinuities occur in the extrema plots as indicated by the dashed vertical lines. At 50 K the value $\phi = \pi/2$ is observed. This shows that there is a phase shift of π between the oscillations at 4 and 50 K. This is naturally the same phase difference as observed in Fig. 1. The magnetoresistance at 20 and 30 K shows this phase shift even in a single residual-phase plot.

It is surprising that MIS oscillations occur, although only a single subband is observed at 4 K in the SdH oscillations. Converting the fundamental fields in Table I to energies using Eq. (2.1), $E_{F,1} \lesssim E_{12}$ is found, i.e., the Fermi level is below although close to the second subband energy. The population of the second subband at 4 K is then very small and cannot be measured accurately. However, at 30 K the broadening of the Fermi-Dirac distribution is an order of magnitude larger than at 4 K and a significant thermal population exists in the second subband. As a consequence MIS oscillations can occur. A self-consistent calculation solving the coupled Poisson-Schrödinger equations using the measured n_s gives an agreement within 10% between experimental and theoretical E_{12}. The subband spacing E_{12} determined from $B_{f,MIS}$ is temperature independent between 20 and 100 K, as it is expected for the squarelike potential of this type of heterojunction.

Figure 3 shows the normalized power spectra of the curves in Fig. 1 using the full measured data sets ranging from $B = 0.5$ to 15 T. A single peak and its harmonics are observed at 4 K. An asymmetric peak is observed at 20 K, it splits into two peaks at 30 and 50 K and again a single peak is observed at 100 K. The dotted vertical line is a guide to the eye to assess the positions of the peaks in relation to each other. The absolute peak positions are given in Table I. The fundamental-field values at 30 K are about 7% below and above the value at 4 K. One of the fields at 30 K has to be due to the SdH oscillations observed at high fields in the magnetoresistance in Fig. 1. A power spectrum of the data at 30 K including only the data points up to 4.5 T is shown as the dashed line. It has only a single peak aligned with the dotted vertical line. This shows that the split peak in the power spectrum of the full data set is due to the two regimes in the oscillatory magnetoresistance having a similar B_f with $\Delta\phi \approx \pi$.

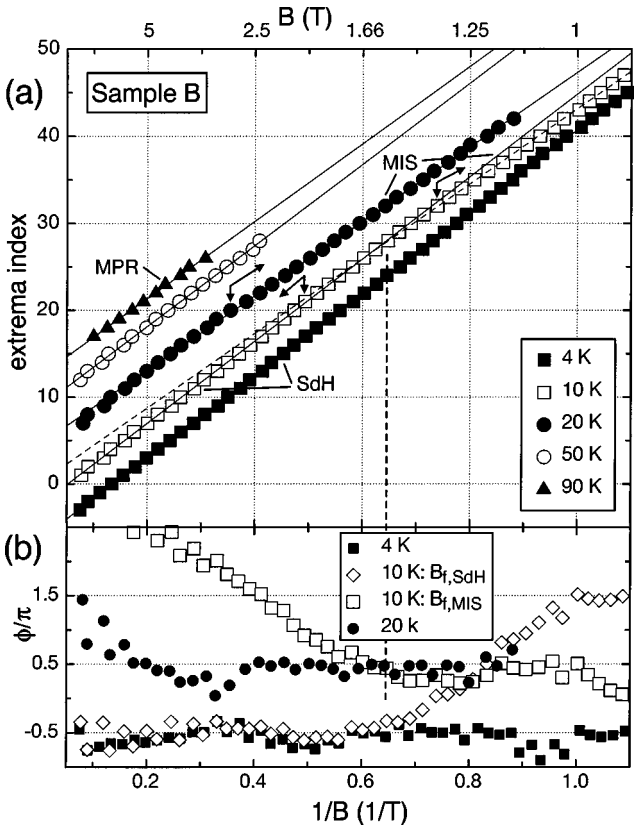

FIG. 4. The extrema-index (a) and residual-phase (b) plots for sample *B*. In (a) two fundamental fields are observed at 10 K. From (b) a phase shift of π between the oscillations at 4 and 20 K can be deduced. At 10 K the phase shift occurs between the low- and high-field oscillations as demonstrated by the phase plots for the two different fundamental fields.

C. Experimental results for sample *B*

After the specific case of sample *A*, we discuss data obtained from a standard $Al_{0.3}Ga_{0.7}As/GaAs$ heterojunction with two populated subbands at 4 K. The magnetoresistance data of sample *B* can be found in Ref. 7 together with preliminary analysis. The SdH oscillations show clearly two occupied subbands after illumination at 4 K. Upon increasing the temperature the magnetoresistance shows a temperature-dependent node similar to sample *A* and oscillations persist in the magnetoresistance above 100 K.

Two linear regions with different slopes corresponding to two different B_f values are resolved at 10 K in the extrema-index plots in Fig. 4(a). The value in the high-field range is similar to the value observed at 4 K as can be seen in Table I and it is associated with the SdH oscillations. The low field B_f is interpreted as the MIS effect. The relation $B_{f,MIS} < B_{f,SdH,1}$ corresponds to $E_{12} < E_{F,1}$. This relation is consistent with the second subband population observed in the SdH effect at 4 K. At 50 and 90 K a single B_f is observed, the

value at 50 K is very close to the SdH value at 4 K. Due to the thermal damping of the SdH effect over the entire magnetic-field range, the oscillations at 50 K can only be the MIS effect. The relation $B_{f,MIS}(T=50\,\mathrm{K})>B_{f,MIS}(T=10\,\mathrm{K})$, i.e., a temperature-dependent subband spacing $E_{12}(50\,\mathrm{K})>E_{12}(10\,\mathrm{K})$, can be explained by the thermal redistribution of carriers in a heterojunction with an approximately triangular potential and two populated subbands. The B_f value at 90 K is close to the magneto phonon resonance (MPR) value in this system.[16] The MPR effect is strong in this system and it can be observed above 50 K.[17] The peak positions observed in power spectra are given in Table I for comparison.

Figure 4(b) shows the residual-phase plots for sample *B* between 4 and 20 K. At 4 K the phase is slightly undulating around $-\pi/2$. This is probably due to the complex nature of the magnetoresistance in the presence of a second populated subband, where all components of Eq. (2.2) are expected to be present. At 10 K two B_f values are observed in the low and high-field region, $B_{f,MIS}$ and $B_{f,SdH}$, respectively, and for each the corresponding phase plot is shown. These two plots are constant only in the mutually exclusive low- and high-field region. The point of deviation from constant phase coincides with the change in slope in Fig. 4(a) as indicated by the dashed vertical line. The phase in the high-field region (low $1/B$) is $\phi=-\pi/2$ and in the low-field region $\pi/2$. At 20 K the phase is $\pi/2$ with some deviations in the high-field region. Therefore, $\Delta\phi=\pi$ is observed in sample *B* between the SdH at 4 K and the MIS oscillations at higher temperatures similar to sample *A*, the only difference to sample *A* is a different B_f value of the two effects.

V. CONCLUSIONS

By studying the magnetoresistance in an $Al_{0.3}Ga_{0.7}As/GaAs$ heterojunction and an $Al_{0.3}Ga_{0.7}As/In_{0.15}Ga_{0.85}As/GaAs$ quantum well with high carrier concentrations at temperatures above 4 K, we have isolated unambiguously a phase difference $\Delta\phi\approx\pi$ between SdH and MIS oscillations in strong support of the theory. The phase difference is best observed between 10 and 50 K, where the oscillatory magnetoresistance shows a node separating the MIS oscillations at low fields from the SdH oscillations at high fields. This node is a consequence of the interplay between the temperature damping of the SdH oscillations and the phase difference between SdH and MIS oscillations. The phase difference is estimated directly from the extrema positions in the oscillatory magnetoresistance and from residual phase plots. It is found that the phase difference can lead to a split peak in the power spectrum of oscillatory data. The two samples studied correspond to the cases $E_{F,1}\lesssim E_{12}$ and $E_{F,1}>E_{12}$ at 4 K. Nevertheless, the MIS oscillations observed at higher temperatures show similar behavior for both samples due to the thermal redistribution of the carriers.

Other systems reported in the literature with two (or several) populated subbands, which seem suitable to investigate further the MIS effect, include $In_{0.53}Ga_{0.47}As/InP$ heterojunctions,[15] $Al_{0.52}In_{0.48}As/In_{0.53}Ga_{0.47}As/InP$ quantum wells,[14,18] and $Al_{0.71}In_{0.29}As/In_{0.3}Ga_{0.7}As$ heterojunctions.[11]

Our work is relevant to low-temperature magnetoresistance data published some years ago[19,20] and more recently.[21] Nodes in the oscillatory magnetoresistance as shown in Fig. 1 are observed in $Al_{0.52}In_{0.48}As/In_xGa_{1-x}As$ quantum wells at temperatures below 4 K. These have been attributed to zero-field spin splitting.[21] From the magnetoresistance data given in the reference the absolute population of the second subband was estimated to be as high as $n_{s,2}\approx 4.5\times10^{11}\,\mathrm{cm}^{-2}$. From earlier work[5] it is known that the MIS effect is present at 0.55 K in an $Al_{0.3}Ga_{0.7}As/GaAs$ heterojunction with two populated subbands and it seems possible that the data in Ref. 21 is influenced by the MIS effect. Any effect related to spin-splitting should exhibit the same temperature damping and the same phase as the SdH oscillations.

The power spectra of the oscillatory magnetoresistance in InAs/GaSb quantum wells with two subbands show clear evidence of the MIS effect.[22] The MIS effect and a finite zero magnetic-field spin-splitting due to the spin-orbit term[23,24] both lead to beating in the low-field Shubnikov–de Haas oscillations in this material combination. The dominance of the spin-orbit coupling can be critical for spin-electronic devices and understanding the regime where the MIS effect can dominate the low-field magnetoresistance is important in this field of electronics.

ACKNOWLEDGMENTS

We thank Professor R. A. Stradling for helpful discussions. T.H.S. acknowledges the support of the EPSRC/UK (Grant No. GR/J 97540) and of the EU under its ''Access to large scale facilities'' scheme.

*Present address: Kirchenhoelzle 17, 79104 Freiburg, Germany.

†Present address: Toshiba Cambridge Research Center Ltd., Cambridge CB4 4WE, United Kingdom.

‡Present address: University College, Dept. of Electrical Engineering, London WC1E 7JE, United Kingdom.

[1] A. Isihara and L. Smrčka, J. Phys. C **19**, 6777 (1986).

[2] H. L. Störmer, A. C. Gossard, and W. Wiegmann, Solid State Commun. **41**, 707 (1982).

[3] J. J. Harris, D. E. Lacklinson, C.T. Foxon, F. M. Selten, A. M. Suckling, R. J. Nicholas, and K. W. J. Barnham, Semicond. Sci. Technol. **2**, 783 (1987).

[4] P. T. Coleridge, Semicond. Sci. Technol. **5**, 961 (1990).

[5] D. R. Leadley, R. Fletcher, R. J. Nicholas, F. Tao, C. T. Foxon, and J. J. Harris, Phys. Rev. B **46**, 12 439 (1992).

[6] M. E. Raikh and T. V. Shahbazyan, Phys. Rev. B **49**, 5531 (1994).

[7] T. H. Sander, S. N. Holmes, J. J. Harris, D. K. Maude, and J. C. Portal, Surf. Sci. **361/362**, 564 (1996).

[8] R. Fletcher, J. J. Harris, and C. T. Foxon, J. Phys. C **3**, 3479 (1991).

[9] S. E. Schacham, E. J. Haugland, and S. A. Alterovitz, Phys. Rev. B **45**, 13 417 (1992).

[10] E. Skuras, R. Kumar, R. L. Williams, R. A. Stradling, J. E. Dmochowski, E. A. Johnson, A. Mackinnon, J. J. Harris, R. B. Beall, S. Skierbeszewski, J. Singleton, P. J. van der Wel, and P. Wisniewski, Semicond. Sci. Technol. **6**, 535 (1991).

[11] J. Chen, H. H. Wieder, and A. P. Young, J. Appl. Phys. **76**, 4743 (1994).
[12] P. T. Coleridge, Phys. Rev. B **44**, 3793 (1991).
[13] A. Kastalsky, R. Dingle, K. Y. Cheng, and A. Y. Cho, Appl. Phys. Lett. **41**, 274 (1982).
[14] Y. Guldner, J. P. Vieren, M. Voos, F. Delahaye, D. Dominguez, J. P. Hirtz, and M. Razeghi, Phys. Rev. B **33**, 3990 (1986).
[15] W. H. Press, B. P. Flannery, S. A. Teukolsky, and W. T. Vetterling, *Numerical Recipes — The Art of Scientific Computing* (Cambridge University Press, Cambridge, 1986).
[16] R. J. Nicholas, Prog. Quantum Electron. **10**, 1 (1985).
[17] G. Gregoris, J. Beerens, S. B. Amor, L. Dmowski, J. C. Portal, F. Alexandre, D. L. Sivco, and A. Y. Cho, Phys. Rev. B **37**, 1262 (1988).
[18] J. C. Portal, R. J. Nicholas, M. A. Brummel, A. Y. Cho, K. Y. Cheng, and T. P. Pearsall, Solid State Commun. **43**, 907 (1982).
[19] B. Das, D. C. Miller, S. Datta, R. Reifenberger, W. P. Hong, P. K. Bhattacharya, J. Singh, and M. Jaffe, Phys. Rev. B **39**, 1411 (1989).
[20] B. Das, S. Datta, and R. Reifenberger, Phys. Rev. B **41**, 8278 (1990).
[21] J. Nitta, T. Akazaki, H. Takayanagi, and T. Enoki, Phys. Rev. Lett. **78**, 1335 (1997).
[22] T. A. Malik, S. J. Chung, R. A. Stradling, W. T. Yuen, J. J. Harris, and A. G. Norman, in *Narrow Gap Semiconductors 1995*, edited by J. L. Reno, IOP Conf. Proc. No. 144 (Institute of Physics, London, 1995), p. 229.
[23] J. Luo, H. Munekata, F. F. Fang, and P. J. Stiles, Phys. Rev. B **41**, 7685 (1990).
[24] E. A. de Andrada e Silva, G. C. La Rocca, and F. Bassani, Phys. Rev. B **50**, 8523 (1994).